THE JOURNAL OF PHYSICAL CHEMISTRY A

Article

pubs.acs.org/JPCA

Spectral-to-Temporal Amplitude Mapping Polarization Spectroscopy of Rotational Transients

Erin T. McCole,[†,§] Johanan H. Odhner,[†,§] Dmitri A. Romanov,[‡,§] and Robert J. Levis*[,†,§]

[†]Department of Chemistry, [‡]Department of Physics, and [§]Center for Advanced Photonics Research, Temple University Philadelphia, Pennsylvania 19122, United States

ABSTRACT: A new implementation of pump−probe polarization spectroscopy is presented where the revivals of an impulsively excited rotational wavepacket are mapped onto a broad-band, chirped continuum pulse to measure a long temporal window without the need for delay scanning. Experimental measurements and a theoretical framework for spectral−temporal amplitude mapping polarization spectroscopy (STAMPS) as applied to impulsive rotational motion are presented. In this technique, a femtosecond laser pulse is used to prepare a rotational wavepacket in a gas-phase sample at room temperature. The rotational revivals of the wavepacket are then mapped onto a chirped continuum (400−800 nm) pulse created by laser filamentation in argon. Nearly single-shot time-resolved rotational spectra are recorded over a 65 ps time window. The transient birefringence spectra are simulated by including terms for polarization rotation of the probe as well as cross-phase modulation. Measurements and simulations are presented for the cylindrically symmetric N_2, O_2, and CO_2 molecules. The long time window of the method allows measurement of rotational spectra for asymmetric top molecules, and here we present measurements for ethylene and methanol.

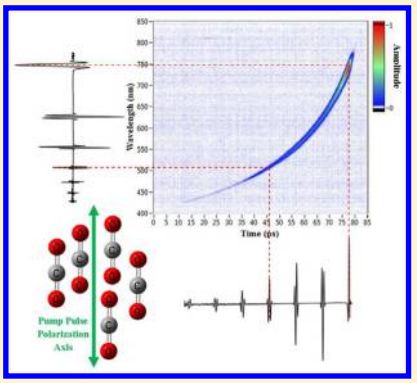

INTRODUCTION

Laser-induced, field-free rotational wavepacket alignment was predicted in 1971[1] and first observed experimentally in 1975 by the same group[2] using a polarization-gate geometry to detect the transient birefringence induced by CS_2 revivals. In general, molecules experience postpulse periodic molecular alignment, often referred to as rotational revivals[3] or field-free molecular alignment,[4] when subjected to an intense, ultrashort laser pulse. This nonadiabatic alignment occurs when the condition $T_p \ll T_r$ is fulfilled, where T_p is the pulse duration of the exciting laser pulse, $T_r = 1/(2Bc)$ is the rotational period of the molecule, $B = h/(8\pi^2 Ic)$ is the molecular rotational constant, I is the moment of inertia for the respective molecule, and c is the speed of light. This can be understood as the simultaneous excitation of populated rotational states of a molecule through Raman transitions, which prepares a coherent superposition of states (a rotational wavepacket). The wavepacket subsequently will undergo frequency-spread dephasing[5] and then will rephase at fractional and integer multiples of the rotational period. Classically, in the case of a homonuclear diatomic molecule, initial molecular alignment will occur along the polarization axis of the exciting laser pulse. After the laser pulse is gone, the molecules rotate out of alignment. As long as the rotational coherence of the molecules is preserved (i.e., collisional dephasing is negligible), alignment will recur. The degree of rotational alignment depends on the polarizability of the molecule, which in turn is a function of molecular structure. For linear and symmetric top molecules, a rotational wavepacket can fully rephrase, because these molecules have a single available molecular axis for rotation.[6]

Asymmetric top molecules have three molecular axes that are defined by the Euler angles (θ, χ, ϕ) with respect to the polarization axis and propagation direction of the laser pulse. The molecular axes have different values of the associated moments of inertia and polarizabilities, thus allowing for alignment of the molecule in three dimensions.[4,7−10] The torque applied by a strong, linearly polarized electric field to an asymmetric top molecule always affects at least two axes of the molecule.[6] Overall, the evolution of rotational wavepackets in asymmetric top molecules is much more complex than for linear or symmetric top molecules, and the components of the wavepacket never fully rephase, making detection of asymmetric top molecules a challenge. Furthermore, the moments of inertia in such molecules are typically large, resulting in long revival periods, which make measurements at long delay times (>10 ps) particularly important.

Coulomb explosion imaging,[11] transient birefringence,[12] spectral interferometry,[13,14] spatial focusing/defocusing,[15,16] and degenerate four-wave mixing[17,18] are among the methods that have been developed and used to study field-free molecular alignment. Most of these methods involve scanning the temporal delay between pump and probe pulses to investigate molecular motion in the wake of the pump pulse. This requires precise optical alignment over the desired scan length to avoid spatial walk-off when the delay time is scanned. In addition,

Special Issue: Prof. John C. Wright Festschrift

Received: March 1, 2013
Revised: May 6, 2013
Published: May 6, 2013

   dx.doi.org/10.1021/jp402135t | J. Phys. Chem. A 2013, 117, 6354−6361

making such measurements can be data intensive and time-consuming, especially for molecules whose revival times are on the order of tens to hundreds of picoseconds after initial excitation.[19−22]

Single-shot measurements of the rotational wavepacket motion can also be used to probe the time-dependent response. Several methods for conducting single-shot measurements of rotational revivals have been developed thus far.[14,23−25] Zamith et al. performed transient birefringence measurements where the rotational alignment initiated by a weak, unfocused pump beam was detected with a 50 fs probe pulse chirped to 500 fs.[23] Spectral interferometry studies were conducted in which a pump pulse excites a rotational wavepacket that is detected using a pair of chirped probe pulses.[14,24] A spatial imaging technique was applied to the measurement of rotational revivals by Loriot et al.,[25] who monitored the spatial birefringence induced on an unfocused probe beam during its interaction with the rotational wakes generated by an orthogonally focused pump beam.

Here we present a new technique for performing rotational spectroscopy using impulsive excitation. The method is based on chirping the coherent white-light continuum generated in a laser filament to map the temporal dynamics of a rotational wavepacket through birefringence and cross-phase modulation. We investigate the temporal rotational response for N_2, O_2, CO_2, ethylene, and methanol over a time period of 65 ps in two nonscanning measurements, affording direct access to the temporal evolution of a wavepacket in a relatively small molecule. Probing the rotational motion in real time is otherwise difficult, as the rotational transitions have low frequencies and normally require narrow-band, or long laser pulses to resolve in a single measurement.

EXPERIMENTAL SECTION

The transient birefringence of various gaseous samples was measured using a polarization gate pump−probe scheme, as illustrated in Figure 1. A Ti:sapphire amplifier, producing 2.5 mJ, 52 fs (with a Fourier-transform limit of 38 fs) pulses at a 1 kHz repetition rate and having a nominal central wavelength of 800 nm, is used to generate a strong pump beam (up to 575 μJ) and a weak probe beam (>1 μJ). The probe beam is generated

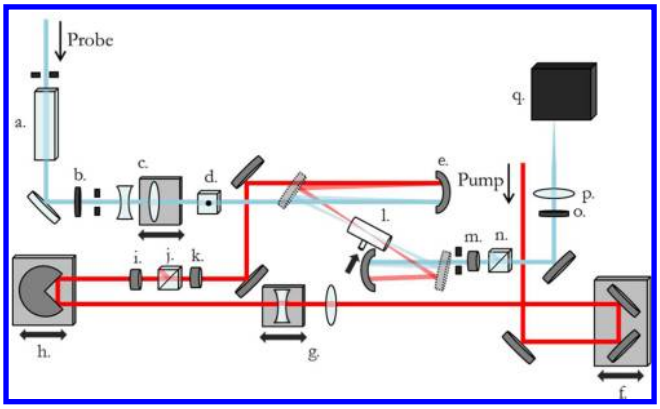

Figure 1. STAMPS experimental scheme: (a) SF11 glass block; (b) short pass filter <750 nm; (c) beam expander; (d) and (j) polarizing cube; (e) 25 cm spherical mirror; (f) mechanical delay stage; (g) beam reducer; (h) electronic delay stage; (i) and (k) half-wave plate; (l) sample tube; (m) quarter-wave plate; (n) polarizing cube (analyzer); (o) color glass filter; (p) 10 cm lens; (q) spectrometer.

by loosely focusing a 750 μJ pulse with an f = 2.07 m lens to generate a filament in an open-ended tube. Argon is leaked into the tube at a sufficient rate to displace the air and lower the threshold required for filamentation. Filamentation in argon results in blue-side spectral broadening to ∼300 nm with a well-behaved spectral phase in the visible and ultraviolet portion of the spectrum (i.e., no rapid variations in the phase in these spectral regions). A small portion of the white light continuum generated through the filamentation process is isolated with an optical blank and used as a broad-band probe. To reduce spectral interference between the pump and probe pulses around the fundamental (800 nm), a short pass filter is used to remove radiation with wavelength longer than 750 nm. The probe is temporally chirped by an 8.3 cm long block of SF11 glass to extend over ∼65 ps (Figure 2b) and collimated by a telescope. A Glan-laser polarizer ensures the linear polarization of the probe pulse before the interaction region and adds additional dispersion to the probe pulse. The pump beam size is reduced to match the probe beam waist and is sent through a half-wave plate and Glan-laser polarizer to ensure linear pump polarization as well as to control the pump pulse power. A second half-wave plate after the Glan-laser polarizer is used to set the pump polarization at an angle of 45° with respect to the probe. A computer-controlled delay line in the pump beam path facilitates long scans over the duration of the chirped probe pulse to measure the group delay of the probe pulse in the interaction region.

Both beams are focused by a 25 cm spherical mirror into an open sample cell in the shape of a "T", where they cross at a small angle (∼3°) and are subsequently collimated by a second 25 cm spherical mirror. The pulse duration of the pump is estimated to be ∼120 fs fwhm at the sample due to dispersion in the polarizing optics. N_2, O_2, CO_2, and ethylene were directly introduced into the cell, and methanol was introduced by flowing argon through the liquid sample and transporting the vapor to the interaction region. External heating was used to eliminate evaporative cooling of methanol. For N_2, O_2, CO_2, and ethylene, an effective[26] pump intensity range of 2.7×10^{12} to 3.9×10^{12} W/cm^2 was used; however, methanol detection required higher intensities. The effective pump intensity is the intensity $I/1.7$ to account for volume averaging effects in the noncollinear pump−probe geometry used in this investigation.

Any portion of the probe beam undergoing transient polarization rotation in the interaction region passes through the Glan-laser polarizer acting as a cross analyzer and is then focused by a 10 cm lens into a spectrometer (Ocean Optics, USB4000-VIS-NIR). Neutral density filters, along with a color glass filter (KG.5, Schott) that strongly attenuates 800 nm light, prevent saturation in the spectrometer. A zero-order quarter-wave plate (designed for 800 nm) is inserted between the collimating lens and the cross analyzer to produce a local oscillator from the probe field to add either constructively or destructively to the birefringence signal for heterodyne measurements. The quarter-wave plate exhibited a nearly linear response over the continuum wavelength range, as determined by measuring the extinction ratio of the probe through the crossed polarizers with the wave plate at 0°. As outlined in Figure 2, spectra were acquired with and without the pump beam in the presence of the local oscillator and dividing the pump-on spectra by the pump-off spectra yielded intensity normalized signal spectra. Conversion of the frequency domain signal to the time domain was achieved by mapping the frequency axis onto the time axis using the group delay of the

dx.doi.org/10.1021/jp402135t | J. Phys. Chem. A 2013, 117, 6354−6361

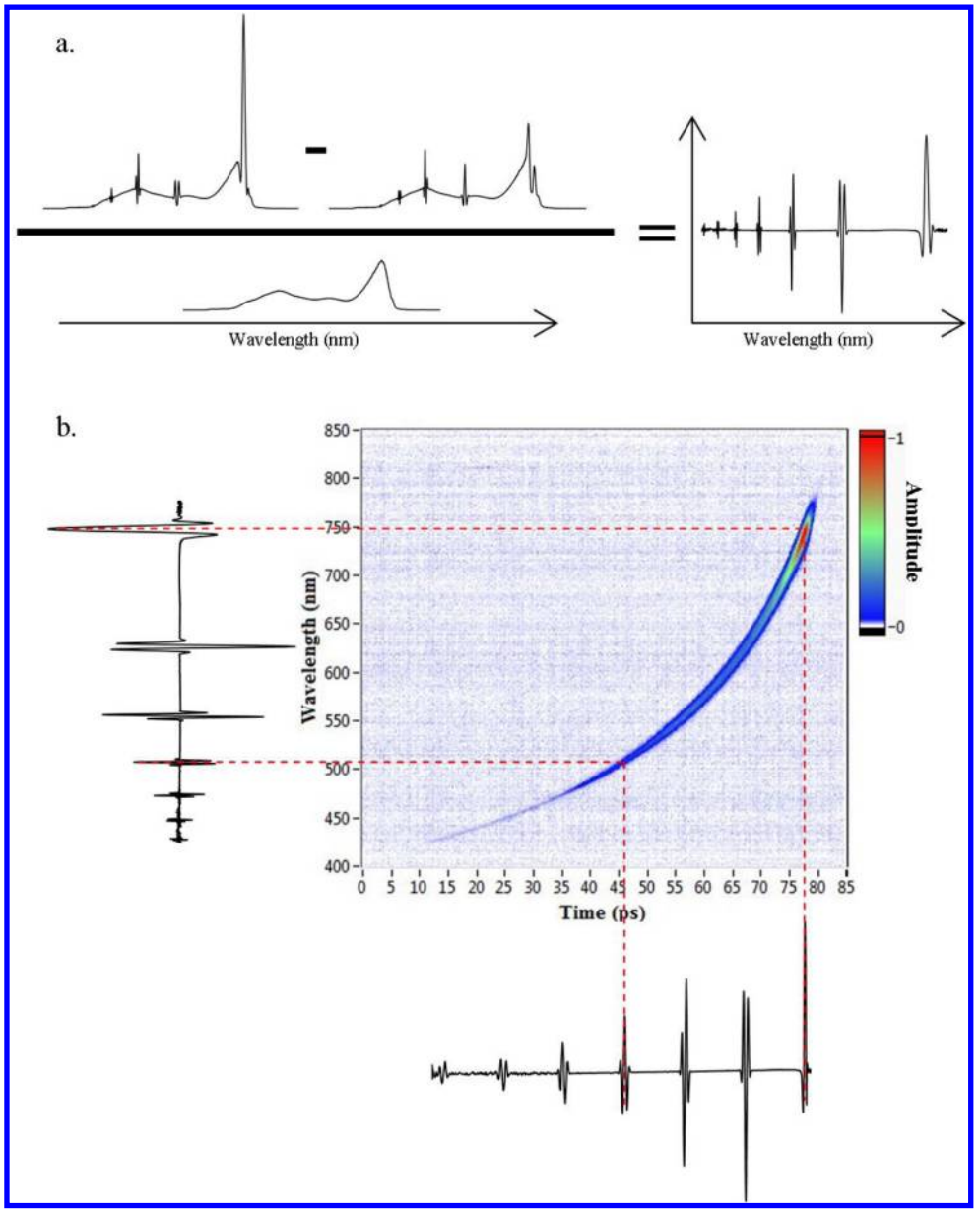

Figure 2. Diagrammatic representation of the procedure used to process the STAMPS signal and convert from the spectral domain to the temporal domain. (a) The pump-on heterodyned spectra are subtracted ((+heterodyne) − (−heterodyne)) and subsequently divided by the pump-off spectrum to yield a pure heterodyne (background-free) spectrum. (b) The spectral signal is then mapped onto the temporal domain using the measured probe pulse group delay.

probe pulse, measured by cross-correlating the pump and probe pulses in argon in situ and detecting in a homodyne configuration.

THEORY

The frequency-resolved heterodyned signal, $I_{het}(\omega)$, measured in the detection configuration described in the previous section is proportional to

$$I_{het}(\omega) \propto \frac{\mathrm{Re}[E_{LO}(\omega)\, E_s^*(\omega)]}{|E_{pr}(\omega)|^2} \tag{1}$$

in analogy with the time-domain expression for the integrated heterodyne birefringence signal,[27] where $E_{LO}(\omega) = e^{i\theta}E_{pr}(\omega)$, $E_{pr}(\omega)$, and $E_s(\omega)$ are the Fourier components of the local oscillator (derived from the probe), the incident probe, and the signal electric fields, respectively.[27,28] Unlike scanning pump−probe transient birefringence measurements, the spectral density of the probe pulse changes as a function of time, requiring that the heterodyne signal be normalized by the probe spectral density to properly reconstruct the amplitude of the birefringence signal. The signal, $E_s(\omega)$, can be approximated as

$$E_s(\omega) = \frac{-iz\omega_c}{n_0 c}\int_{-\infty}^{\infty}(\Delta n_{el}(t) + \Delta n_{rot}(t))E_{pr}(t)e^{-i\omega t}\,dt \tag{2}$$

where

$$\Delta n_{el}(t) = \frac{2}{3}n_2(1-\kappa)\, I_{pu}(t)$$

dx.doi.org/10.1021/jp402135t | J. Phys. Chem. A 2013, 117, 6354−6361

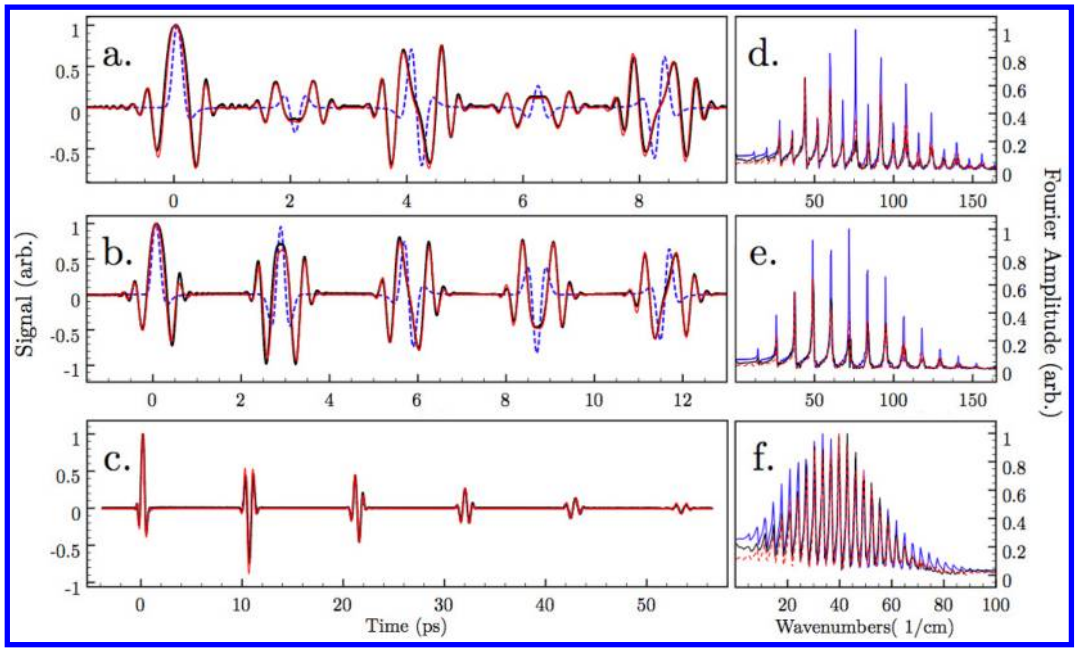

Figure 3. Measurements and simulations of the STAMPS signal in nitrogen (a), oxygen (b), and carbon dioxide (c). The corresponding Fourier spectra are shown in (d), (e), and (f), respectively. Experimental data: black lines. Simulated line shapes: red lines. Calculated induced-phase modulation from rotational revivals: dotted blue lines.

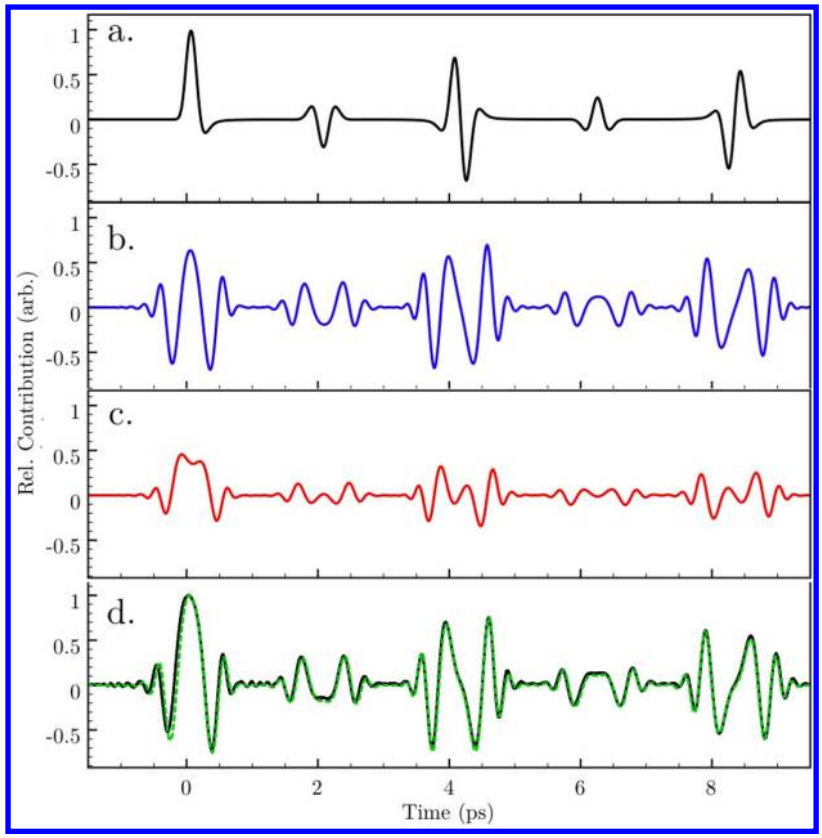

Figure 4. For nitrogen, a comparison of the calculated induced change in the refractive index (a), with the calculated XPM contribution (b), the calculated birefringence contribution (c), and the measured (black solid line) and simulated (green dashed line) signals (d), where the simulated signal is the sum of the XPM and birefringence contributions (i.e., the total nitrogen signal).

$$\Delta n_{\mathrm{rot}}(t) = \frac{3}{2} n_2 \kappa \int_{-\infty}^{t} R(t-t')\, I_{\mathrm{pu}}(t')\, \mathrm{d}t' \qquad (3)$$

z is the propagation distance in the interaction region, ω_c is the carrier frequency of the probe pulse, n_2 is the nonlinear refractive index at ω_c, $I_{\mathrm{pu}}(t)$ is the temporal intensity profile of the pump pulse, κ is a scaling constant for the relative responses of the electronic and rotational Kerr responses, and $R(t)$ is the rotational response function calculated by summing over the

dx.doi.org/10.1021/jp402135t | J. Phys. Chem. A 2013, 117, 6354−6361

molecular rotational transitions excited through the Raman process.[29−32] Note that with respect to the weak probe field, the response in eq 3 is instantaneous and linear. Thus, no nonlinear propagation of the probe need be taken into account. We have neglected dispersion in the nonlinear refractive index, as considerable growth of n_2 occurs at much higher frequencies than measured here[33] (see ref 33 and references therein). All simulations are normalized with respect to amplitude, leaving the relative contributions of the instantaneous and delayed responses through κ and the temperature and collisional dephasing time in the rotational response function as adjustable parameters. The relative contributions of the instantaneous and delayed responses for N_2 and O_2 were taken from ref 32, whereas for CO_2 κ is taken empirically to be 0.9. We have neglected the grating-induced contribution to the signal that results from optical interference between the pump and probe pulses coupled through the Kerr, rotational, and plasma generation effects, as this contribution is only manifested when the pump and probe pulses are degenerate, which is not the case here.[28,34,35] We have also disregarded the vibrational contribution to the change in refractive index, as the pump pulse at the sample is long compared to the vibrational periods of the molecules under study. The birefringence is modeled by substituting eqs 2 and 3 into eq 1 and using the probe pulse spectrum, measured in the spectrometer, and the probe pulse phase extracted from the group delay measured by cross-correlating the pump and probe pulses in argon. The pump pulse is simulated using a chirped 45 fs Gaussian pulse with bandwidth centered at 800 nm.

RESULTS AND DISCUSSION

Spectral-temporal amplitude-mapping polarization spectroscopy measurements of nitrogen, oxygen, and carbon dioxide are shown in Figure 3a−c, respectively. Unlike previous scanning birefringence measurements of rotational revivals in nitrogen and oxygen, the STAMPS response has additional modulations at the times anticipated for fractional revivals as shown by the solid black lines in Figure 3a,b. The theoretical signal calculated using eq 1 is shown as the red lines in Figure 3 and is in good agreement with the data for all molecules measured, confirming that both birefringence and cross-phase modulation (XPM) must be taken into account, in the form of the local oscillator phase, to correctly interpret the STAMPS signal. The change in refractive index induced by the rotational revivals alone can be calculated directly in the time domain and is shown as blue dashed lines in Figure 3.

To further elucidate the origin of the STAMPS signal response, Figure 4 shows the relative contributions of XPM and birefringence to the total signal of nitrogen, isolated by calculating the in-phase and out-of-phase contributions of the local oscillator, respectively. Cross-phase modulation clearly dominates but cannot account for the signal alone. The presence of cross-phase modulation in the signal is due to the large spectral chirp of the probe pulse and can be qualitatively understood in terms of the uncertainty relation.[36] When the temporal feature being imprinted on the chirped probe contains a structure whose Fourier transform contains more frequency components than are present in the probe pulse itself at that point in time, local spectral broadening occurs, which interferes with adjacent spectral (temporal) slices. This suggests that longer-duration rotational revival structures, requiring fewer Fourier components to describe the signal in the time domain, will result in less modulation in the retrieved STAMPS signal. Therefore, less modulation will be observed in larger molecules (for a given probe pulse chirp), because larger molecules rotate more slowly and have slower transients. To test whether the degree of interference present in the signal depends on the rotational revival time, we measured the STAMPS response for CO_2. The STAMPS measurement of carbon dioxide (Figure 3c) is nearly indistinguishable from the induced refractive index change (blue dashed line) calculated from the rotational response, with the exception of the instantaneous Kerr response at zero delay, which still leads to noticeable modulation of the signal due to the short duration of the pump pulse.

The Fourier transform of the STAMPS measurement also affords insight into its information content compared with pump−probe scanning polarization spectroscopy measurements. Parts d−f of Figure 3 show the Fourier transforms of the curves shown in Figure 3a−c for nitrogen, oxygen, and carbon dioxide, respectively. The Fourier spectrum largely reflects the expected rotational Raman spectrum. The interference from XPM filters the amplitudes of the spectral components but does not contribute additional components to the frequency domain spectrum. This allows for the evaluation of the interlevel spacing from the measured rotational spectra, which for nitrogen, oxygen, and carbon dioxide are measured to be 7.98, 11.49, and 3.12 cm^{-1}. These values agree well with the calculated values of 7.99, 11.50, and 3.12, respectively.[37,38]

The full STAMPS measurement of CO_2 is shown in Figure 5, demonstrating a temporal measurement range of 65 ps. This

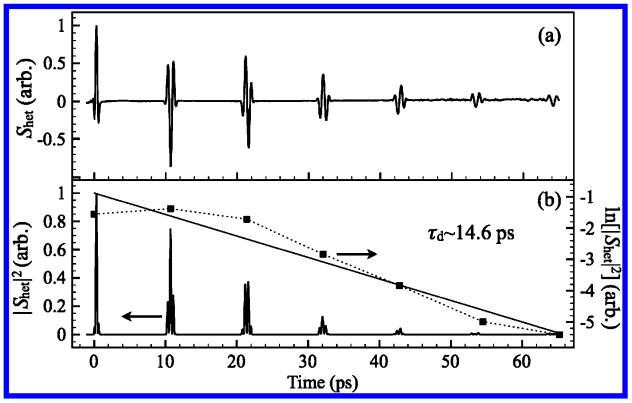

Figure 5. (a) Measured STAMPS signal of CO_2 demonstrating a temporal measurement range of 65 ps. (b) Magnitude-square of the signal shown in (a) (left scale) and the natural log of the integrated peak intensities and the linear fit of the log values (right scale). The dephasing time calculated in this manner is 14.6 ps.

molecule has been studied previously using both scanning[39] and single-shot[24] phase-sensitive geometries. In agreement with previous measurements[12,40,41] we observe a rotational period of 42.8 ps for CO_2, with a quarter rotational period of $T_{partial} = T_r/4 \approx 10.7$ ps. The decrease in signal intensity of the CO_2 revivals as a function of delay is mainly the result of collisional dephasing, which destroys the coherence of the wavepacket. The decline in signal may also arise from linear filtering due to the fact that different wavelengths contained in the probe pulse are focused to different beam waists in the geometry used (a result of the spatial distribution of spectral components generated in the filamentation process).[42] The collisional dephasing time was calculated by taking the magnitude-square of the heterodyne signal and integrating the revival peaks

dx.doi.org/10.1021/jp402135t | J. Phys. Chem. A 2013, 117, 6354−6361

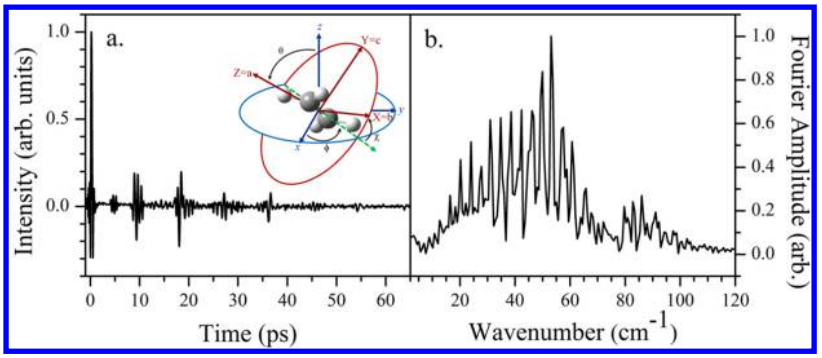

Figure 6. (a) STAMPS signal of ethylene and (b) the Fourier transform of the signal shown in (a). Inset: an ethylene molecule in the laboratory-fixed frame with respect to the Euler angles.

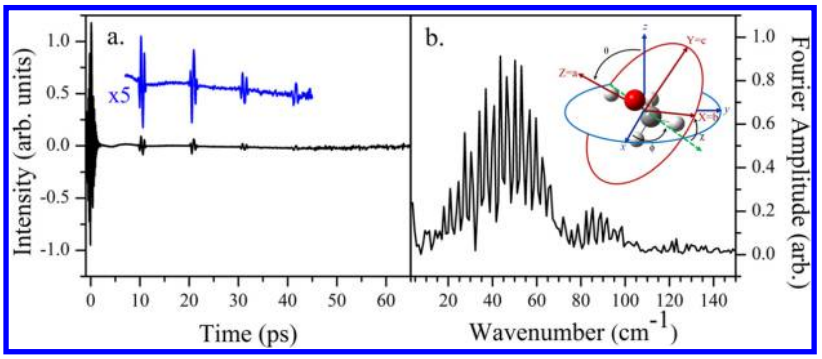

Figure 7. (a) STAMPS signal of methanol with revivals shown at x5 (blue) and (b) the Fourier transform of the signal shown in (a). Inset: a methanol molecule plotted with respect to the Euler angles.

(Figure 5), which yields a dephasing time of $\tau_d \sim 14.6$ ps. The dephasing time used in the simulation to match the heterodyne signal intensity (Figure 4) was $\tau_d = 15.1$ ps, which is in reasonable agreement with the calculated value. Both of these dephasing times are significantly shorter than the reported value of collisional dephasing in CO_2 at STP, previously measured to be 30 ps.[17] This presumably is due to the decreased sampling volume in the blue wavelengths in the filament probe beam in comparison with the red wavelengths and may also partially be explained by the fact that the measurement is made in a flow cell, where the local pressure is somewhat higher. Further quantitation of the exact focusing conditions of the beam along with more sophisticated numerical simulations are under way.

STAMPS was also used to investigate the rotational response of two asymmetric-top molecules, ethylene and methanol. Ethylene is nearly a symmetric top molecule but is classified as an asymmetric top (having D_{2h} symmetry), because it has a minor rotational axis defined by its four hydrogen atoms. Thus, its rotational evolution pattern is expected to resemble that of a symmetric top case, superimposed by fast transients related to rotation with respect to the minor axis. The STAMPS measurement of ethylene is shown in Figure 6a and is consistent with previously reported measurements.[4,8,43−45] *J*- and *C*-type rotational transients are observed in an asymmetric top like ethylene. *J*-type transients correspond to rotation of the major molecular axis toward the direction of laser polarization, which is the only type that exists for linear molecules and symmetric tops. *C*-type transients correspond to rotation about the *c*-axis and are only observed in asymmetric top molecules.[43,46] The molecular axes (*X*, *Y*, *Z*) of ethylene are defined and the molecule is represented with respect to the Euler angles of rotation in the laboratory-fixed frame (*x*, *y*, *z*, the *z*-axis being along the polarization of the pump laser field, and the *x*-axis being along the pump wavevector) in the inset of Figure 6a. The STAMPS signal of ethylene exhibits strong interference because the transients contain structures that change rapidly in time, as noted previously. Still, the Fourier transform of the signal, shown in Figure 6b, provides insight into the rotational constants and rotational line spacing of ethylene. The interlevel spacing is measured to be 3.69 cm^{-1}, which is in agreement with a calculation of 3.68 cm^{-1} for the S-branch transitions using the effective rotational constant $\tilde{B}$ = 0.911 cm^{-1} reported by Gallaway and Barker.[47] For nearly symmetric top molecules, the effective rotation constant is defined as $\tilde{B} = {}^1/_2(B + C)$.[38]

As a prototypical measurement of a molecule with even lower symmetry, STAMPS was also used to investigate the rotational response of methanol, and the result is presented in Figure 7a. To achieve detectable signal levels in methanol vapor, the effective pump intensity was increased to 1.6×10^{13} W/cm^2. The small signal is due to the low Raman scattering cross-section, in part a consequence of a noncylindrical shape (as shown in the inset to Figure 7b), and also the lower concentration of methanol in the detection region due to the method of vapor delivery. Methanol is considered slightly asymmetric, having a C_s symmetry (assuming a staggered configuration), and as such it does not mimic a symmetric top molecule as well as ethylene. The significantly lower STAMPS signal intensity of methanol in comparison with ethylene partly results from its lower relative symmetry. The three available rotational axes of methanol preclude complete rephasing of the rotational wavepacket after the initial alignment. To the best of our knowledge, the field-free molecular alignment of methanol

dx.doi.org/10.1021/jp402135t | J. Phys. Chem. A 2013, 117, 6354−6361

has never been experimentally measured; so to evaluate the temporal accuracy of the revival structures, we again utilize the Fourier transform of our measurement, shown in Figure 7b. The dominant line spacing is found to be 3.21 cm^{-1}, which matches the calculated spacing of 3.21 cm^{-1} determined using the effective rotational constant $\tilde{B}$ = 0.8032 cm^{-1} reported by Borden and Barker,[48] confirming the accuracy of the measurement.

We note that it is possible to achieve 3D alignment of asymmetric top molecules by varying the ellipticity of the exciting laser pulse or using multiple excitation pulses with different polarizations.[4,7,8] Three-dimensional alignment of asymmetric molecules using an elliptically polarized pump pulse was first performed adiabatically[7,9] and has subsequently been demonstrated using nonadiabatic excitation.[4] Elliptically polarized pulses facilitate alignment along the major axis of the molecule as well as a minor molecular axis, leading to higher signal intensities and allowing for control of the transient realignments. Underwood et al. theoretically investigated the utility of using elliptically polarized excitation pulses versus double pulse excitation and calculated that excitation by two time-delayed, orthogonally polarized pulses yields better resolved transient features.[8] Therefore, a combination of multipulse excitation and manipulation of the pump pulse polarization could prove to be another method of increasing the STAMPS sensitivity.

CONCLUSION

In this work, we have presented nearly single-shot measurements of rotational coherences over an unprecedented 65 ps range. The pump−probe scheme was employed as a means to detect several symmetric linear molecules, including diatomics, and several asymmetric top molecules. The capability of the STAMPS method to make rapid measurements over such long time scales should prove useful for rapid temperature and pressure measurements as well as for other applications in time-resolved spectroscopy for tracking chemical events. The added complexity of the spectral modulations that unavoidably accompany the STAMPS measurement complicates analysis, but we have shown here that it is possible to fully reconstruct the signal, providing a possible route for extracting the underlying molecular dynamics.

AUTHOR INFORMATION

Corresponding Author

*E-mail: rjlevis@temple.edu. Telephone: (215) 204-5241.

Notes

The authors declare no competing financial interest.

ACKNOWLEDGMENTS

We acknowledge the generous support of the Office of Naval Research through N00014-10-0293 and the Defense Threat Reduction Agency through HDTRA1-12-0014 for this research.

REFERENCES

(1) Lin, C. H.; Heritage, J. P.; Gustafson, T. K. Susceptibility Echos in Linear Molecular Gases. *Appl. Phys. Lett.* **1971**, *19*, 397−400.

(2) Heritage, J. P.; Gustafson, T. K.; Lin, C. H. Observation of Coherent Transient Birefringence in CS_2 Vapor. *Phys. Rev. Lett.* **1975**, *34*, 1299−1302.

(3) Seideman, T. Revival Structure of Aligned Rotational Wave Packets. *Phys. Rev. Lett.* **1999**, *83*, 4971−4974.

(4) Rouzee, A.; Guerin, S.; Faucher, O.; Lavorel, B. Field-Free Molecular Alignment of Asymmetric Top Molecules Using Elliptically Polarized Laser Pulses. *Phys. Rev. A* **2008**, *77*, 043412/1−043412/8.

(5) Lucht, R. P.; Roy, S.; Meyer, T. R.; Gord, J. R. Femtosecond Coherent Anti-Stokes Raman Scattering Measurement of Gas Temperatures from Frequency-Spread Dephasing of the Raman Coherence. *Appl. Phys. Lett.* **2006**, *89*, 251112/1−251112/3.

(6) Faucher, O.; Lavorel, B.; Hertz, E.; Chaussard, F. Optically Probed Laser-Induced Field-Free Molecular Alignment. In *Progress in Ultrafast Intense Laser Science Vii*; Yamanouchi, K.;, Charalambidis, D., Normand, D., Eds.; Springer: Berlin, Heidelberg, 2011; Vol. *100*, pp 79−108.

(7) Larsen, J. J.; Hald, K.; Bjerre, N.; Stapelfeldt, H.; Seideman, T. Three Dimensional Alignment of Molecules Using Elliptically Polarized Laser Fields. *Phys. Rev. Lett.* **2000**, *85*, 2470−2473.

(8) Underwood, J. G.; Sussman, B. J.; Stolow, A. Field-Free Three Dimensional Molecular Axis Alignment. *Phys. Rev. Lett.* **2005**, *94*, 143002/1−143002/4.

(9) Tanji, H.; Minemoto, S.; Sakai, H. Three-Dimensional Molecular Orientation with Combined Electrostatic and Elliptically Polarized Laser Fields. *Phys. Rev. A* **2005**, *72*, 063401/1−063401/4.

(10) Nevo, I.; Holmegaard, L.; Nielsen, J. H.; Hansen, J. L.; Stapelfeldt, H.; Filsinger, F.; Meijer, G.; Kupper, J. Laser-Induced 3D Alignment and Orientation of Quantum State-Selected Molecules. *Phys. Chem. Chem. Phys.* **2009**, *11*, 9912−9918.

(11) Rosca-Pruna, F.; Vrakking, M. J. J. Experimental Observation of Revival Structures in Picosecond Laser-Induced Alignment of I_2. *Phys. Rev. Lett.* **2001**, *87*, 153902/1−153902/4.

(12) Renard, V.; Renard, M.; Guerin, S.; Pashayan, Y. T.; Lavorel, B.; Faucher, O.; Jauslin, H. R. Postpulse Molecular Alignment Measured by a Weak Field Polarization Technique. *Phys. Rev. Lett.* **2003**, *90*, 153601/1−153601/4.

(13) Hartinger, K.; Bartels, R. A. Pulse Polarization Splitting in a Transient Wave Plate. *Opt. Lett.* **2006**, *31*, 3526−3528.

(14) Chen, Y. H.; Varma, S.; York, A.; Milchberg, H. M. Single-Shot, Space- and Time-Resolved Measurement of Rotational Wavepacket Revivals in H_2, D_2, N_2, O_2, and N_2O. *Opt. Express* **2007**, *15*, 11341−11357.

(15) Renard, V.; Faucher, O.; Lavorel, B. Measurement of Laser-Induced Alignment of Molecules by Cross Defocusing. *Opt. Lett.* **2005**, *30*, 70−72.

(16) Wu, J.; Cai, H.; Tong, Y.; Zeng, H. Measurement of Field-Free Molecular Alignment by Cross-Defocusing Assisted Polarization Spectroscopy. *Opt. Express* **2009**, *17*, 16300−16305.

(17) Frey, H. M.; Beaud, P.; Gerber, T.; Mischler, B.; Radi, P. P.; Tzannis, A. P. Femtosecond Nonresonant Degenerate Four-Wave Mixing at Atmospheric Pressure and in a Free Jet. *Appl. Phys. B: Laser Opt.* **1999**, *68*, 735−739.

(18) Ren, X.; Makhija, V.; Kumarappan, V. Measurement of Field-Free Alignment of Jet-Cooled Molecules by Nonresonant Femtosecond Degenerate Four-Wave Mixing. *Phys. Rev. A* **2012**, *85*, 033405/1−033405/6.

(19) Connell, L. L.; Corcoran, T. C.; Joireman, P. W.; Felker, P. M. Observation and Description of a New Type of Transient in Rotational Spectroscopy. *J. Phys. Chem.* **1990**, *94*, 1229−1232.

(20) Felker, P. M. Rotational Coherence Spectroscopy - Studies of the Geometries of Large Gas-Phase Species by Picosecond Time-Domain Methods. *J. Phys. Chem.* **1992**, *96*, 7844−7857.

(21) Jarzeba, W.; Matylitsky, V. V.; Riehn, C.; Brutschy, B. Rotational Coherence Spectroscopy of Jet-Cooled Molecules by Femtosecond Degenerate Four-Wave Mixing: Non-Rigid Symmetric and Asymmetric Tops. *Chem. Phys. Lett.* **2003**, *368*, 680−689.

(22) Poulsen, M. D.; Peronne, E.; Stapelfeldt, H.; Bisgaard, C. Z.; Viftrup, S. S.; Hamilton, E.; Seideman, T. Nonadiabatic Alignment of Asymmetric Top Molecules: Rotational Revivals. *J. Chem. Phys.* **2004**, *121*, 783−791.

(23) Zamith, S.; Ansari, Z.; Lepine, F.; Vrakking, M. J. J. Single-Shot Measurement of Revival Structures in Femtosecond Laser-Induced Alignment of Molecules. *Opt. Lett.* **2005**, *30*, 2326−2328.

(24) Hartinger, K.; Bartels, R. A. Single-Shot Measurement of Ultrafast Time-Varying Phase Modulation Induced by Femtosecond Laser Pulses with Arbitrary Polarization. *Appl. Phys. Lett.* **2008**, *92*, 021126/1−021126/3.
(25) Loriot, V.; Tehini, R.; Hertz, E.; Lavorel, B.; Faucher, O. Snapshot Imaging of Postpulse Transient Molecular Alignment Revivals. *Phys. Rev. A* **2008**, *78*, 013412/1−013412/7.
(26) Loriot, V.; Bejot, P.; Ettoumi, W.; Petit, Y.; Kasparian, J.; Henin, S.; Hertz, E.; Lavorel, B.; Faucher, O.; Wolf, J. P. On Negative Higher-Order Kerr Effect and Filamentation. *Laser Phys.* **2011**, *21*, 1319−1328.
(27) Lavorel, B.; Tran, H.; Hertz, E.; Faucher, O.; Joubert, P.; Motzkus, M.; Buckup, T.; Lang, T.; Skenderovi, H.; Knopp, G.; et al. Femtosecond Raman Time-Resolved Molecular Spectroscopy. *C. R. Phys.* **2004**, *5*, 215−229.
(28) Odhner, J. H.; Romanov, D. A.; McCole, E. T.; Wahlstrand, J. K.; Milchberg, H. M.; Levis, R. J. Ionization-Grating-Induced Nonlinear Phase Accumulation in Spectrally Resolved Transient Birefringence Measurements at 400 nm. *Phys. Rev. Lett.* **2012**, *109*, 065003/1−065003/5.
(29) Zheltikov, A. M. An Analytical Model of the Rotational Raman Response Function of Molecular Gases. *J. Raman Spectrosc.* **2008**, *39*, 756−765.
(30) Lin, C. H.; Heritage, J. P.; Gustafson, T. K.; Chiao, R. Y.; McTague, J. P. Birefringence Arising from Reorientation of Polarizability Anisotropy of Molecules in Collisionless Gases. *Phys. Rev. A* **1976**, *13*, 813−829.
(31) Ripoche, J. F.; Grillon, G.; Prade, B.; Franco, M.; Nibbering, E.; Lange, R.; Mysyrowicz, A. Determination of the Time Dependence of N_2 in Air. *Opt. Commun.* **1997**, *135*, 310−314.
(32) Nibbering, E. T. J.; Grillon, G.; Franco, M. A.; Prade, B. S.; Mysyrowicz, A. Determination of the Inertial Contribution to the Nonlinear Refractive Index of Air, N_2, and O_2 by Use of Unfocused High-Intensity Femtosecond Laser Pulses. *J. Opt. Soc. Am. B* **1997**, *14*, 650−660.
(33) Brée, C.; Demircan, A.; Steinmeyer, G. Kramers-Kronig Relations and High-Order Nonlinear Susceptibilities. *Phys. Rev. A* **2012**, *85*, 033806/1−033806/8.
(34) Wahlstrand, J. K.; Milchberg, H. M. Effect of a Plasma Grating on Pump-Probe Experiments near the Ionization Threshold in Gases. *Opt. Lett.* **2011**, *36*, 3822−3824.
(35) Wahlstrand, J. K.; Odhner, J. H.; McCole, E. T.; Cheng, Y.-H.; Palastro, J. P.; Levis, R. J.; Milchberg, H. M. Effect of two-beam coupling in strong-field optical pump-probe experiments. *Phys. Rev. A* **2013**, *87*, 053801/1−053801/13.
(36) Kim, K. Y.; Alexeev, I.; Milchberg, H. M. Single-Shot Supercontinuum Spectral Interferometry. *Appl. Phys. Lett.* **2002**, *81*, 4124−4126.
(37) Herzberg, G. Spectra of Diatomic Molecules In *Molecular Spectra and Molecular Structure*, 2nd Ed.; Krieger Publishing Co.: Malabar, FL, 1989; Vol. *I*.
(38) Herzberg, G. Infrared and Raman Spectra of Polyatomic Molecules In *Molecular Spectra and Molecular Structure*, 2nd ed.; Krieger Publishing Co.: Malabar, FL, 1989; Vol. *II*.
(39) Lavorel, B.; Faucher, O.; Morgen, M.; Chaux, R. Analysis of Femtosecond Raman-Induced Polarization Spectroscopy (RIPS) in N_2 and CO_2 by Fitting and Scaling Laws. *J. Raman Spectrosc.* **2000**, *31*, 77−83.
(40) Bartels, R. A.; Weinacht, T. C.; Wagner, N.; Baertschy, M.; Greene, C. H.; Murnane, M. M.; Kapteyn, H. C. Phase Modulation of Ultrashort Light Pulses Using Molecular Rotational Wave Packets. *Phys. Rev. Lett.* **2001**, *88*, 013903/1−013903/4.
(41) Renard, V.; Renard, M.; Rouzee, A.; Guerin, S.; Jauslin, H. R.; Lavorel, B.; Faucher, O. Nonintrusive Monitoring and Quantitative Analysis of Strong Laser-Field-Induced Impulsive Alignment. *Phys. Rev. A* **2004**, *70*, 033420/1−033420/9.
(42) Gallmann, L.; Pfeifer, T.; Nagel, P. M.; Abel, M. J.; Neumark, D. M.; Leone, S. R. Comparison of the Filamentation and the Hollow-Core Fiber Characteristics for Pulse Compression into the Few-Cycle Regime. *Appl. Phys. B: Laser Opt.* **2007**, *86*, 561−566.
(43) Rouzee, A.; Guerin, S.; Boudon, V.; Lavorel, B.; Faucher, O. Field-Free One-Dimensional Alignment of Ethylene Molecule. *Phys. Rev. A* **2006**, *73*, 033418/1−033418/9.
(44) Rouzee, A.; Boudon, V.; Lavorel, B.; Faucher, O.; Raballand, W. Rotational Raman Spectroscopy of Ethylene Using a Femtosecond Time-Resolved Pump-Probe Technique. *J. Chem. Phys.* **2005**, *123*, 154309/1−154309/6.
(45) Xu, N.; Wu, C.; Ma, R.; Huang, J.; Wu, Z.; Liang, Q.; Yang, H.; Gong, Q. Dynamic Alignment of C_2H_4 Investigated by Using Two Linearly Polarized Femtosecond Laser Pulses. *J. Am. Soc. Mass. Spectrom.* **2006**, *17*, 1717−1724.
(46) Holmegaard, L.; Viftrup, S. S.; Kumarappan, V.; Bisgaard, C. Z.; Stapelfeldt, H.; Hamilton, E.; Seideman, T. Control of Rotational Wave-Packet Dynamics in Asymmetric Top Molecules. *Phys. Rev. A* **2007**, *75*, 051403/1−051403/4.
(47) Gallaway, W. S.; Barker, E. F. The Infra-Red Absorption Spectra of Ethylene and Tetra-Deutero-Ethylene under High Resolution. *J. Chem. Phys.* **1942**, *10*, 88−97.
(48) Borden, A.; Barker, E. F. The Infra-Red Absorption Spectrum of Methyl Alcohol. *J. Chem. Phys.* **1938**, *6*, 553−563.